Title: Improved peroxide biosensor based on Horseradish Peroxidase/Carbon Nanotube on a thiol-modified gold electrode

Authors: A.K.M. Kafi, M. Naqshabandi, Mashitah M. Yusoff, Maxwell J. Crossley

PII: S0141-0229(17)30211-9
DOI: https://doi.org/10.1016/j.enzmictec.2017.11.006
Reference: EMT 9156

To appear in: *Enzyme and Microbial Technology*

Received date: 11-10-2017
Revised date: 13-11-2017
Accepted date: 14-11-2017

Please cite this article as: Kafi AKM, Naqshabandi M, Yusoff Mashitah M, Crossley Maxwell J.Improved peroxide biosensor based on Horseradish Peroxidase/Carbon Nanotube on a thiol-modified gold electrode.*Enzyme and Microbial Technology* https://doi.org/10.1016/j.enzmictec.2017.11.006

Improved peroxide biosensor based on Horseradish Peroxidase/Carbon Nanotube on a thiol-modified gold electrode

A.K.M. Kafi[a]*, M. Naqshabandi[b], Mashitah M. Yusoff[a], Maxwell J. Crossley[b]

[a]*Faculty of Industrial Sciences & Technology, Universiti Malaysia Pahang*,Kuantan 26300, Malaysia

[b]School of Chemistry, The University of Sydney, Sydney, NSW, *Australia*

* Corresponding author. Tel.:+609 549 2392, Fax: +609 549 2766
Email: kafiakm@ ump.edu.my

Graphical Abstract

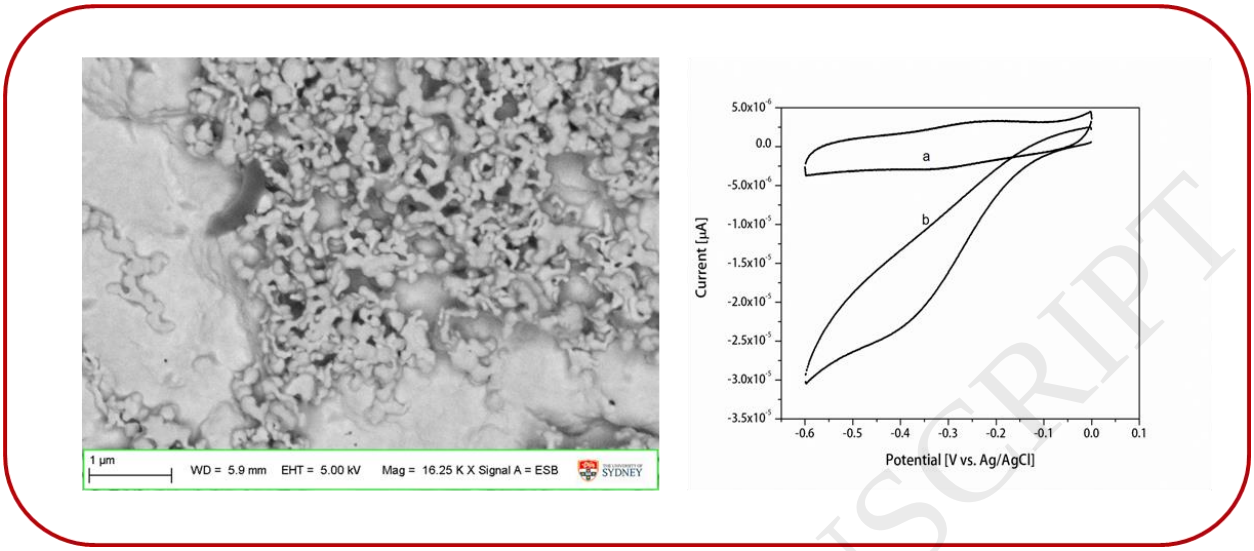

Highlights

- For quick understanding about the importance of the work following are the significant findings of our submitted article.
- We have described a novel approach to build a three dimensional conductive networks of crosslinked HRP/carbon nanotube on Thiol-modified Au electrode electrochemically. Establishing efficient electrical communication between biomolecules and the electrode is the most challenging task for a bioelectronics system. In this network, these elements are integrated by cross-linking with a short conductive electron relay unit causing the whole system to be much more electro-responsive than previous work by others. Electrical contact between HRP and the electrode is achieved successfully and exhibited higher current response than the previous studied. The key innovation is that this leads to a general new concept in sensing and that the matrices that are produced are made cheaply and reliably in a short time. Furthermore because the active centers are never far from a conductive element there is a very fast response time in the sensing, seconds rather than hours of other systems. The constructed HRP/carbon nanotube network on gold nanotube arrays exhibits high conductivity by expediting the electrical transfer from HRP to the Au electrode and has a high electrocatalytic property for sensing hydrogen peroxide (H_2O_2). A longer linear range, low LOD and very quick response time in the sensing are really noteworthy. We believe that the paper opens up new avenues in the field of enzyme based biosensors/bioelectronics.

Abstract

A new 3-dimensional (3D) network of crosslinked Horseradish Peroxidase/Carbon Nanotube (HRP/CNT) on a thiol-modified Au surface has been described in order to build up the effective electrical wiring of the enzyme units with the electrode. The synthesized 3D HRP/CNT network has been characterized with

cyclic voltammetry and amperometry which results the establishment of direct electron transfer between the redox active unit of HRP and the Au surface. Electrochemical measurements reveal that the high biological activity and stability is exhibited by the immobilized HRP and a quasi-reversible redox peak of the redox centre of HRP was observed at about −0.355 and −0.275 V *vs*. Ag/AgCl. The electron transfer rate constant, K_S and electron transfer co-efficient α were found as 0.57 s^{-1} and 0.42, respectively. Excellent electrocatalytic activity for the reduction of H_2O_2 was exhibited by the developed biosensor. The proposed biosensor modified with HRP/CNT 3D network displays a broader linear range and a lower detection limit for H_2O_2 determination. The linear range is from 1.0×10^{-7} to 1.2×10^{-4} M with a detection limit of $2.2.0\times10^{-8}$M at 3σ. The Michaelies–Menten constant *K*app M value is estimated to be 0.19 mM. Moreover, this biosensor exhibits very high sensitivity, good reproducibility and long-time stability.

Keywords: Three-dimensional networks; HRP; Carbon nanotube; Direct electron transfer; Biosensors; Hydrogen peroxide

1. Introduction

The electrochemical investigation of redox active enzyme/protein at solid electrode is one of the main challenges and is of great importance for developing products in electronics applications. Intact redox active enzymes contain one or more redox active subunits embedded in a well-defined polypeptide structures [1]. The electrochemically active redox centers of the enzyme are located deep inside the insulated shells which makes the direct electron transfer (DET) as a challenging task. A new route to biosensor and bioelectronics devices has been opened by DET between redox active enzymes and metal electrodes and the direct electrochemical synthesis of biochemical is the fundamental interest of many researchers [2]. Proceeding ahead with this type of research requires advanced tools and reliable approaches and led to the recognition that an appropriate 'matrix' is essential for providing an interface for the study of electrochemical properties of redox active enzymes and other biomolecules.

Despite of enormous interest in developing devices and advancing applications that include a redox active enzyme-electrode interface, the lack of efficient electrical communication between the redox enzyme and the electronic elements has been a major obstacle observed in a number of recent studies [3-5]. A lot of publications have reviewed the direct electrical communication between the redox centre of an enzyme and conventional metal electrodes recently [6-8]. DET between enzyme and solid substrate is advantageous because it minimizes the problems associated with the use of mediators, such as toxicity, high cost and poor stability. DET strongly depends on the distance between redox active cofactor of enzyme and the collector of electron. To ensure that all redox cofactor units of enzyme are oriented in an optimal position in respect to the conductive supports, and shortening the long electron tunneling distance is a challenge in the development of this area. Adding small redox mediators is a common way to achieve DET, which can diffuse into and out of the enzyme active site, conveying reducing and oxidizing equivalents with them [9]. However, there are several disadvantages in this system such as high cost,

toxicity and diffusion of untethered mediators away from redox enzyme. Controlled orientations of redox enzyme on an electrode surface and their effective electrical wiring by the reconstitution technique have been proven to be successful approach as an alternative [10-12]. Despite of acquiring high electron-transfer turnover rates in those systems, the formation of monolayer of enzyme on the surface of electrodes is a major disadvantage to the method, as a result of the low content of enzyme associated with the surface. All these results come from the low electrical communication caused by the weak contact of the enzymes to the electrode. Using of nanomaterial to give three dimensional (3D) structures to enzymes is one of the attractive solutions to the constraints of existing problem for electronic coupling and communication between the enzymes and the electrode [13-14]. Integration of nanomaterials and redox enzyme has become popular during investigations on the DET between enzymes and solid electrode due to the unique properties of nanomaterials [15-18]. Some limitations can be overcome by nanoscale surfaces such as nanotubes or nanoparticles because they contain regions of high curvature that energetically limit biomolecules adsorption, and reduced steric hindrance of the substrate to binding site on the enzyme. Recently, an excellent method has been reported by us to generate three-dimensional electrically wired Hemoglobin (Hb) electrodes by which high electron-transfer turnover rates have been showed [19]. In this system, a three-dimensional bis-aniline-crosslinked CNT/Hb network has been created by 4-aminothiophenol-modified Hb in the presence of 4-aminothiophenol-functionalized carbon nanotube (CNT). The resulting bis-aniline crosslinked network was redox active and was able to medicate the electron from redox site of Hb to the base electrode.

The present work aims to study the kinetics of direct electron transfer of horseradish peroxidase using the ideas and techniques used by us. Like Hb, the access to the HRP active site is difficult because of the existence of a narrow channel, which naturally makes hindrance to the direct electron transfer (DET) between the electrode and the redox active site of HRP [20]. HRP is a heme enzyme with a molar weight

of ~ 44 kDa which has the ability to catalyze the oxidation of a wide variety of substrates by H_2O_2. In addition, it has been reported that the reduced form of HRP can be reoxidized chemically by H_2O_2 [21].

The focus in the present paper is on the construction of three-dimensional (3-D) conductive HRP network with CNT onto the thiol-modified gold (Au) electrode. CNTs modified with electropolymerizable aniline and 4-aminothiophenol-modified HRP were coelectroplolymerized on the thiol-modified Au electrode surface in order to obtain the 3-D network. Results of this study demonstrate for the first time that the created 3-D HRP/CNT composite effectively builds a good electrical communication between the redox centers of the HRP and an electrode. A H_2O_2 biosensor has been developed based on this bearing in mind that the sensitive and accurate H_2O_2 detection is of great interest to researchers because of having importance in the pharmaceutical, clinical and industrial settings [22].

2. Experimental

2.1 Reagents and materials

Single-walled carbon nanotubes, 4-aminothiophenol, 1-(3-dimethylaminopropyl)-3-ethylcarbodiimide hydrochloride (EDC) were purchased from Aldrich. HRP was purchased from Sigma, used as received and stored at 4 ^{o}C. *N*- (**ε**-Maleimidocaproyloxy) sulfosuccinimide ester (sulfo-EMCS) was purchased from PIERCE (Through Thermofisher).*N*-hydroxysulfosuccinimide sodium salt (NHS) was obtained from Sigma. 30% Hydrogen peroxide was purchased from Fluka and the stock solution of H_2O_2 was diluted from this. All experimental solutions were prepared fresh by appropriate dilution of the stock solutions. All other reagents were of analytical grade and used as supplied. The pure water (18 MΩ. cm) that was used to prepare all the solutions in this study was purified with the Nanopure® water system. All the experiments were performed in 0.1 mol l^{-1} phosphate buffer solutions (PBS) whose pH values were adjusted with K_2HPO_4 and KH_2PO_4.

2.2 Modification of HRP and CNT

The functionalization of HRP and CNT was accomplished based on the method previously used by us [19]. Firstly, 50 mg of HRP was dissolved in 0.1M phosphate buffer (3 mL, pH 7.4). Then the solution was treated with *N*-(**ε**-Maleimidocaproyloxy) sulfosuccinimide ester (sulfo-EMCS, 50 μl of 10mg/ml) and stirred for 40 min. The solution was then mixed with 4-aminothiophenol (4-aminothiophenol) and left for 2.5 h. Finally, the solution was eluted through a G-25 column (GE Healthcare) with 0.1m phosphate buffer (pH 7.4) as the eluent. The resulting purified, functionalized HRP solution was lyophilized to yield a powder that was stored at -20 ^{0}C. On the contrary, CNTs were sonicated for 10 h in a mixture solution of concentrated sulfuric acid and nitric acids (3:1) prior to modification which results the oxidization of CNTs. The oxidized CNTs were washed with water and centrifuged several times until the final pH is 7.0. The CNTs were then reacted with a HEPES buffer, 0.01 M, pH = 7.4, containing 2-(4 aminophenyl)-ethylamine and was stirred with 1-(3-dimethylaminopropyl)-3-ethylcarbodiimide hydrochloride (EDC) and *N*-hydroxysulfosuccinimide sodium salt (NHS) for 2 h at room temperature. The modified CNTs were thoroughly rinsed with water finally and centrifuged for at least four times, using a PBS solution.

2.3 Fabrication of 3-D HRP/CNT network on 4-aminothiophenol-modified Au electrode

In this study, we have used a gold (Au) electrode (2 mm diameter) in the fabrication of 3-D CNT/Hb network. The Au electrode was electrocycled ranging between -0.1 and +1.1 V (versus Ag/AgCl) in solution containing H_2SO_4 prior to build 3D networks to remove any contaminations and was immersed in ethanol before monolayer assembly. The cleaned Au-electrode was modified by immersion in a solution of 50 mM 4-aminothiophenol in ethanol. To ensure a complete coverage, the Au electrode was thoroughly rinsed with ethanol and dried under a stream of nitrogen after 24 hours. Electropolymerization was then done on this modified Au-electrode with modified CNTs and HRP in 0.1M phosphate buffer (pH 7.4) by using a fixed number of repetitive cyclic voltammetry scans, ranging between -0.1 and +1.1 V (*vs*. Ag/AgCl), at a

scan rate of 100 mVs^{-1}. The resulting modified Au electrode is mentioned below as Au/SAM/HRP/CNT. Another electrode Au/SAM/HRP was also modified for comparison. In addition, a gold thin film was prepared by electroless deposition method describes elsewhere [18]. This Au thin film was used for morphological characterization of 3D networks film.

2.4 Instrumentations and electrochemical measuring procedures

In this study, all electrochemical experiments were performed using a CHI (660B) workstation. Cyclic voltammetry and amperometric experiments were carried out in a conventional one-compartment cell with a three-electrode configuration holding 20 ml of supporting electrolyte (phosphate buffer). Three electrodes consist of the Au/SAM/HRP/CNT electrode or the Au/SAM/HRP electrode as the working, a platinum coil as a counter electrode, and a KCl saturated Ag/AgCl electrode as a reference electrode were used. The working electrode was cycled in a 0.1 mol l^{-1} PB solution for cyclic voltammetry by applying voltage in the range between 0.0 to -0.8 V vs. Ag/AgCl. Amperometric measurements were performed by applying a potential of -0.4 V to the working electrode in a stirred cell. A magnetic stirrer was used for this experiment. All electrolytes were deoxygenated prior to measurements by bubbling ultra-pure nitrogen for 30 min and maintained under nitrogen atmosphere during the course of the experiment. All measurements were performed at room temperature.

3. Results and discussions

3. 1 Schematic diagram of construction of the 3-D HRP/CNT network

The schematic diagram of the procedures to assemble the HRP/CNT composite electrode is shown in Schematic 1 (Supplementary S1). First of all, 4-aminothiophenol was attached to HRP with the primary modification of the lysine residue of the HRP with the bifunctional *N*-(ε-Maleimidocaproyloxy) sulfosuccinimide ester (sulfo-EMCS), followed by the substitution of the maleimide residue with 4-aminothiophenol (A). Single-wall carbon nanotubes (SWCNTs) were carboxyl functionalized in a mixture

of HNO_3 and H_2SO_4 for 10 h. This functionalized CNTs were then covalently coupled to 2-(4 aminophenyl)-ethylamine (B) using the water-soluble carbodiimide, (1-(3-(dimethylamino) propyl)-3-ethylcarbodiimide hydrochloride, EDC), to promote amide linkages between the carboxyl-terminated CNTs and the amine group of 2-(4 aminophenyl)-ethylamine. Proteins contain many NH_2-containing groups in the side chains of their polypeptide backbones. Therefore, functionalization of HRP was first done by the interaction between NH_2 group of HRP and COOH group of bifunctionalized *N*-(ε-Maleimidocaproyloxy) sulfosuccinimide ester (sulfo-EMCS) by considering the strong amide-bonding interaction between carbonyl and NH_2 groups,. Finally, co-electropolymerization of aniline modified-CNTs and the 4-aminothiophenol modified-HRP onto the 4-aminothiophenol self-assembled monolayer (SAM) on Au electrode was carried out in 0.1 M phosphate buffer (pH 7.4) by using a fixed number of repetitive cyclic voltammetry scans, ranging between -0.1 and +1.1 V (versus Ag/AgCl), at a scan rate of 100 mVs^{-1}.

3.2 Surface characterization of the CNT-HRP modified Au surface

SEM observation and EDS analysis were used to examine the morphology and composition of the Au/SAM/HRP/CNT electrode. An ordered array of gold thin film were shown in figure 1A. This image of the bare Au thin film electrode showed a smooth and featureless morphology. However, the Au/SAM/HRP/CNT composite film exhibited a net structure in figure 1B. Many netlike structure were found homogeneously distributed on the surface of the Au/SAM/HRP/CNT composite film indicating that HRP molecules were connected with carbon nanotube and built up a 3D networks. Additionally, the EDS spectrum (data not shown here) of an Au/SAM/HRP/CNT electrode. Au, O and C peaks are observed in the EDS spectrum of the sample.

3.3 Electrochemical behavior of HRP in the 3-D conductive HRP/CNT networks

Cyclovoltammograms (CV) of the different electrodes recorded in order to investigate the direct electrochemistry attributed to Hb in 3-D HRP/CNT networks in a potential range between -0.6 and 0.0 V

with pH 7.0 PBS at scan rate of 0.05 V/s. CV of different modified Au electrodes were showed in Figure 2. No redox peaks is observed at Au gold electrode and Au/SAM electrode. A small redox peaks which is attributable to HRP is observed at the Au/SAM/HRP electrode, showing that electron transfer between HRP and the Au electrode occurs very slowly. Point to be noted that a well-defined reversible redox peak was observed at the Au/SAM/HRP/CNT electrode, located at about −0.355 and −0.275 V, cathodic and anodic respectively. Electrochemistry of HRP is well behaved at HRP/CNT network at the Au/SAM electrode indicating that CNT on the electrode surface could act as 'promoter' of electron transfer in the electrochemistry of HRP at the Au electrode. At the same time, it can be said that all electroactive heme proteins at HRP/CNT networks have been reduced on the forward cathodic scan, with full conversion of the reduced proteins back to their oxidized forms on the reversed anodic scan. From the cyclic voltammograms, the formal potential (E0'), which can be calculated from the equation of E0'= (Epa + Epc)/2, was got as -0.310 V, which shifts a bit negatively ca. 35mV when compared to that of HRP in sol–gel-derived ceramic–carbon nanotube nanocomposite film [23]. The peak to peak potential separation (ΔEp) at 100 mV s^{-1} was 0.8 V and the ratio of redox peak current (Ipa/Ipc) was approximately to be 1.0. All these features were characteristic of the reversible electrode process of the Fe (III)/Fe (II) redox couple in HRP molecules suggesting that the direct electron transfer of HRP adsorbed on the surface of HRP/CNT network could be achieved.

Further, the thin film properties of HRP/CNT network have been characterized by standard scan-rate dependency. Figure 3 (A) depicted the typical cyclic voltammograms of the Au/SAM/HRP/CNT electrode at different scan rates in pH 7.0 PBS. As we can observe that, the redox peak currents increased gradually with the increase of the scan rate which means that the electrochemical active HRP Fe(III) that present in the HRP/CNT network was reduced to HRP Fe(II) on the forward scan and on the reverse scan the HRP Fe(II) produced was converted to HRP Fe(III). According to figure 3 (B), the anodic and cathodic peak currents were of similar magnitude and both of them were linearly proportional to scan rate range from

50 to 250 mV/s which suggest that the reaction was a surface-controlled process. Later, we have calculated the average surface concentration of electroactive species which can be calculated based on the equation:

Q=nFAΓ*, where Q is the charge passing through the electrode with full reduction of electroactive HRP molecules in HRP/CNT networks, n is the number of electron, F is Faraday's constants and A is the surface area of electrode [24]. The average surface coverage (Γ) of electroactive HRP was calculated to be 3.1×10^{-10} mol cm^{-2}. According to the following equation [25]:

$$E_p = E_o + \frac{RT}{\alpha nF} ln \frac{RTKs}{\alpha nF} - \frac{RT}{\alpha nF} \ln \upsilon \text{.....(1)}$$

Where α is the electron transfer coefficient, n is the electron transfer number, K_s is the standard electron transfer rate constant, υ is the scan rate, E^0 is the formal potential and R, T and F are gas, temperature and the Faraday's constant. The linear regression equations were calculated as E_p (V) = -0.39-(-0.0241)x. According to this equation the electron transfer coefficient (α) and the electron transfer number (n) could be calculated and the results were got as 0.422 and 0.98, respectively. Therefore, it can be concluded that the redox reaction between HRP and the Au electrode is a single electron process, considering n=1 when $0.3 < \alpha < 0.7$ [26]. Then, electron transfer rate constant, K_s value is calculated to be 0.57 s^{-1}, as the intercept of E_p and formal potential E_0 are known

3.4 Catalytic activity towards H_2O_2

Usually, the HRP immobilized on the surface of electrode could show good electrocatalytic ability. Figure 4 shows the cyclic voltammetric responses of the Au/SAM/HRP/CNT in 0.1 M phosphate buffer solution (pH 7.0) containing 0.1 M KCl in the absence and presence of 1 mM H_2O_2. A pair of well-reversible redox wave with was observed in the absence of H_2O_2, while a well-defined reduction catalytic peak was observed with the disappearance of the oxidation peak after adding H_2O_2 to above solution. The following

equations can be used to explain the catalytic mechanism of the immobilized HRP in HRP/CNT network to H_2O_2 reduction [27]:

HRP (Fe^{3+}) + H_2O_2 → Compound I (Fe^{4+}=O) + H_2O... (2)

Compound I (Fe^{4+}=O) + e^- + H^+ → Compound II.....(3)

Compound II + e^- + H^+ → HRP (Fe^{3+}) +H_2O…… (4)

According to equation 1, HRP reacts with H_2O_2 to form a first intermidiate (compound I), which is a two-equivalent oxidized form with oxyferryl heme and a porphyrin π cation radical. Compound I has catalytic activity and its porphyrin radical abtsracts one electron from the electrode to form a second intermidiate (compound II), which is subsequently reduced back to the native HRP by accepting one electron from the electrode.

3.5 Optimal parameters of biosensors

It is well known that a strong effect on the activity of the HRP is shown by the pH of catalytic medium. Thus, the influence of pH was studied systematically between 4.0 and 9.0 using a constant concentration of H_2O_2. Figure 5(A) shows the amperometric response of the Au/SAM/HRP/CNT electrode at different pH in the presence of 5×10^{-5} mol l^{-1} of H_2O_2. It can be observed that the steady-state current is increased with the increasing of the pH from 3.0 to 6.0; however, the amperometric response is decreased when the pH is increased further. It is already reported in the previous study that the pH range of 6.0 to 7.5 reflects the optimum conditions for enzymatic mediated electrochemical reactions [28]. Because of the maximum amperometric response achieved at pH 6.0, this pH is selected so as to ensure higher sensitivity and stability of the proposed Au/SAM/HRP/CNT biosensor.

The choice of the right detection potential is important to achieve the lowest detection limit and avoid the electrochemical interfering species. Therefore, the effect of applied potential have been studied on

the detection of 5×10^{-5} mol l^{-1} of H_2O_2 in the amperometric experiment. As it is being seen in figure 5 (B) the current responses increased as the applied potential varied between 0.0 and -0.6 V. The maximum response was observed at -0.4 V and the application of more negative potentials up to -0.6 V did not increase the current response. This observation indicates that the more negative the operating potential, the higher sensitivity the H_2O_2 biosensor shows. However, there might be a chance of interference reactions from other electroactive species in the solution at more negative potentials. Therefore, we chose the applied potential of -0.4 V. as the working potential for this proposed the Au/SAM/HRP/CNT biosensor, where the background current is minimized and unexpected interfering reactions of the other electroactive species can be avoided effectively. It has been reported here that the number of electropolymerization cycle does effect on the fabrication of CNT/enzyme 3D network that influenced on the biosensors for H_2O_2 detection [19]. Like previous work on this area, the maximum current response is obtained at the application of 70 electropolymerization cycles on the fabrication of HRP/CNT network.

3.6 Amperometric response, reproducibility and stability of the biosensors

Figure 6 (A) shows the steady-state amperometric response of (a) the Au/SAM/HRP/CNT and (b) the Au/SAM/HRP upon the successive additions of a H_2O_2 solution in PBS under the optimized sensing conditions. For the Au/SAM/HRP/CNT biosensor, the response increases and about 95% the steady-state current were achieved at less than 5 s just after the addition of H_2O_2. However, for the Au/SAM/HRP, much lower current responses were found which suggests that the electrode does not respond rapidly to the change of the substrate concentration in comparison with the respond on the Au/SAM/CNT/HRP. Figure 6 (B) shows the corresponding calibration curves for the Au/SAM/HRP/CNT and the Au/SAM/HRP electrodes. A linear relationship of the current to the concentration of H_2O_2 for the Au/SAM/HRP/CNT was observed between 1×10^{-7} to 1.2×10^{-4} M a correlation coefficient of 0.9997 with 15 successive injections of to 1×10^{-5} M of H_2O_2. The sensitivity of the Au/SAM/HRP/CNT biosensor is extremely high, 0.34 μA/μM. The detection limit is estimated to be 2.2×10^{-8} M H_2O_2 (based on S/N = 3).

The apparent Michaelis–Menten constant Km is calculated from the electrochemical version of the Lineweaver–Burk plot to evaluate the biological activity of the immobilized HRP in the HRP/CNT network, [29].

$$\frac{1}{i_{ss}} = \frac{K_m^{app}}{i_{max}}\frac{1}{C} + \frac{1}{i_{max}} \quad \text{..... (3)}$$

Here the steady-state current after the addition of substrate is represented by i_{ss}, whereas, i_{max} stands for the maximum current measured under saturated substrate condition, and C is the bulk concentration of the substrate. According to our experimental data, Km was evaluated as 0.19 mM calculated from the slope and intercept for the plot of the reciprocals of the steady-state current versus H_2O_2 concentration (Figure 6C). The small Km value indicates that the immobilized HRP in HRP/CNT network possesses high enzymatic activity and that the fabricated biosensor exhibits a high affinity for H_2O_2. By measuring the response over period of 1month the long time stability of the Au/SAM/HRP/CNT biosensor was determined. No significant decrease in H_2O_2 (retained over 95% of its initial response) detection was observed from these experiments while the Au/SAM/HRP/CNT biosensor was stored in a phosphate buffer solution at 4 °C. We have studied the electrode-to-electrode reproducibility of 5 different electrodes in above solutions further, and the relative standard deviation was calculated to be 3.9%. The superior reproducibility could be explained by the fact that the amount of immobilized HRP in HRP/CNT network was consistent. The performance of the Au/SAM/HRP/CNT biosensor developed in this study was compared with other biosensors as shown in Table 1, showing that our proposed biosensor shows excellent performance in terms of linearity, low detection limit and high stability.

Conclusions

The direct electrochemistry of HRP was achieved in this study at the HRP/CNT 3D network onto the Au electrode surface. The conductivity to the HRP/CNT network have been provided by CNTs, the bis-aniline bridging units acted as electron-mediating components for the electron transfer between the enzyme

redox centers and the electrode. In addition, close proximities between the redox centers of HRP and the electron relay units have been yielded by the high surface area of the CNTs, and this led to the effective wiring of the HRP with the electrode. Result of this experiment shows the redox process of immobilized HRP in the HRP/CNT network was found to be a quasi-reversible process and the standard rate constant of the direct electron transfer of HRP was determined to be 0.52 s^{-1}. A H_2O_2 biosensor has been fabricated based on the direct electrochemistry of HRP in this experiment which possesses rapid response, low detection limit with satisfactory linear range, stability, and repeatability. The fabrication approach of the biosensor also has advantages such as enhanced electrocatalysis, ease of construction, efficient preservation of the activity of the enzyme, and effective discrimination to the common interfering species.

Acknowledgments

A.K.M. Kafi acknowledges the Henry Bertie and Florence Mabel Gritton Postdoctoral Fellowship, The University of Sydney. This work was also partially supported by Fundamental Research Grant Scheme (RDU140122) and Universiti Malaysia Pahang (UMP) local research grant (RDU 140389).

References

1 Tanja Noll and Gilbert Noll, Chem. Soc. Rev., **2011**, 40, 3564–3576

2 Wiilner, I.; Katz, E.; Willner, B. *Electroanalysis* **1997**, *9*, 965-977.

3 Hasan, B.; Elias, R.; Mohaddeseh, A.-A.; Ali, H.; Yalda, H. A.; Salimeh, A. *Biosens. Bioelectron,* **2016**, 85, 814-821.

4 Gao, Z.D.; Liu, H.F.; Li, C.Y.; Song, Y.Y. *Chem. Commun.* **2013**, 49, 774-776.

5 Tianrong, Z.; Xinjun, W.; Xianjun, L.; Yang, S.; Wanguo, H. Sensors and Actuators B: Chemical, **2016**, 228,101-108

6 Madalina, M.; Barsan, M.; Emilia, G.; Christopher M.A. Brett. Anal. Chim. Acta, **2015**, 881, 1-23.

7 Chao, C.; Qingji, X.; Dawei, Y.; Hualing, X.; Yingchun, F.; Yueming, T. and Shouzhuo, Y, RSC Adv., **2013**, 3, 4473-4491.

8 Yan, Y.M.; Baravik, I.; Yehezkeli, O.; Willner, I. *J. Phys. Chem. C* **2008**, *112*, 17883-17888.

9 Frew, J. E.; Hill, H. A. O. Eur. J. Biochem. **1988**, 172, 261.

10 Zayats, M.; Willner, B.; Willner, I. *Electroanalysis* **2008**, *20*, 583–601.

11 Fruk, L.; Kuo, C. H.; Torres, E.; Niemeyer, C. M. *Angew. Chem., Int. Ed.* **2009**, *48*, 1550-1574.

12 Willner, I.; Willner, B. *Trends Biotechnol.* **2001**, *19*, 222-230.

13 O. Yehezkeli, Y. M. Yan, I. Baravik, R. Tel-Vered, and I. Willner. *Chem. Eur. J.*, **2009**, *15*, 2674.

14 I. Willner, *Electroanalysis*, **1997**, *9*, 965.

15 Kafi, A.K.M.; Wu, G.; Chen, A. *Biosens. Bioelectron.* **2008**, *24*, 566-571.

16 Yang, Y.; Zeng, H.; Zhang, Q.; Bai, X,; Liu, C.; Zhang, Y.H. *Chemical Physics Letters* **2016**, 658, 259-269.

17 Kafi, A.K.M.; Asieh, A.; Wang, J.; Thomas, D.F.; Chen, A. *Biosens. Bioelectron.* **2010**, *25*, 2458-2463.

18 Hui, L.; Kai, G.; Jing, L.; Yuan, G.; Congyue, D.; Lu, D.; Zhenfeng, Z. *Sensors and Actuators B: Chemical*, **2017**, 238, 249-256.

19 A.K.M. Kafi, M.J. Crossley, Biosensors and Bioelectronics, **2013**, 42, 273-279.

20 Saimon Moraes Silva, Delton Martins Pimentel, Rita de Cássia Silva Luz and Flavio Santos Damos *Int. J. Electrochem. Sci.*, **2012**, 7, 1348 – 1358.

21 Liu, S., Chen, A., 2005. Langmuir 21, 409-8413.

22 Wang, L.; Wang, E. *Electrochem. Commun.* **2004**, *6*, 225-229.

23 Hongjun Chen, Shaojun Dong, Biosensors and Bioelectronics **2007**, 22, 1811–1815.

24 Bard, A.J., Faulkner, L.R., Electrochemical Methods; Wiley; New York, **1980**.

25 Laviron, E., **1979**, J. Electroanal. Chem. 101, 19.

26 Ma, H.Y., Hu, N.F., Rusling, J.F., **2000**. J. Electroanal. Chem. 16, 4969.

27 Yi, X., Ju, H.X., and Chen, H.Y., **2000**. Anal. Biochem. 278, 22-28.

28 Santos, A.S., Pereira, A.C., Sotomayor, M.D.P.T., Tarley, C.R.T., Duran, N., Kubota,

29 L.T., **2007**. Electroanalysis 19, 549-554.

30 Kamin, R.A., Wilson, G.S., **1980**. Anal. Chem. 52, 1198.

31 Wang, Y., Ma, X., Wen, Y., Xing, Y., Zhang, Z., Yang, H., 2010. Biosensors and Bioelectronics, 25, 2442-2446.

32 Chen, H., and Dong, S., **2007**. Biosensors and Bioelectronics 22, 1811-1815.

33 Cao, S., Yuan, R., Chai, Y., Zhang, L., Li, X., Gao, F., **2007**. Bioprocess Biosyst Eng. 30, 71-78.

34 Lei, C.X., Hu, S.Q., Gao, N., Shen, G.L., Yu, R.Q., **2004**. Bioelectrochemistry 65, 33-39.

35 Gao, F., Yuan, R., Chai, Y., Chen, S., Cao, S., Tang, M., **2007**. J. Biochem. Biophys. Methods 70, 407-413.

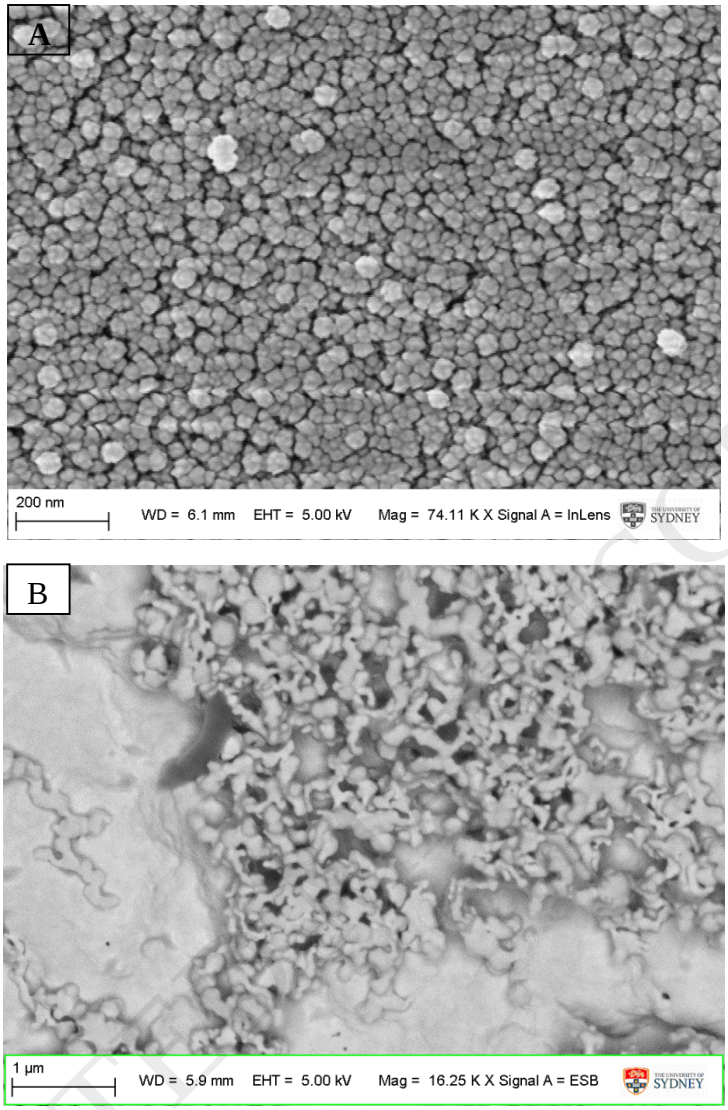

Figure 1. (A) SEM image of Au thin film arrays, (B) SEM of an Au/SAM/HRP/CNT electrode.

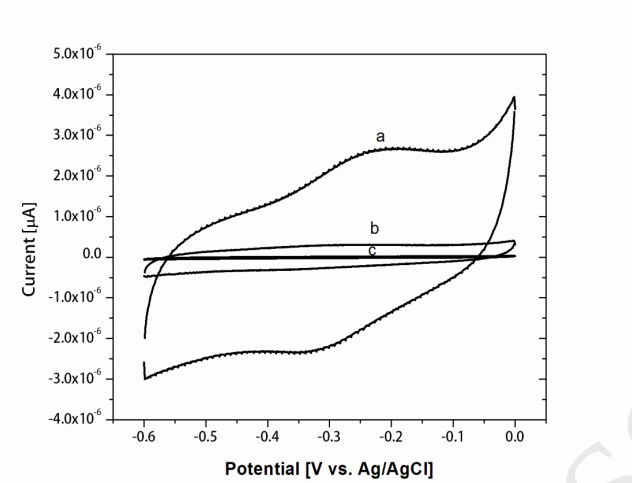

Figure 2. Cyclic voltammamograms response at the Au/SAM/HRP/CNT (a); the Au/SAM/HRP (b) and a bare Au electrode (c) in 0.1 mol l^{-1} PBS with pH 7.0 at a scan rate of 0.1 V/s.

(A)

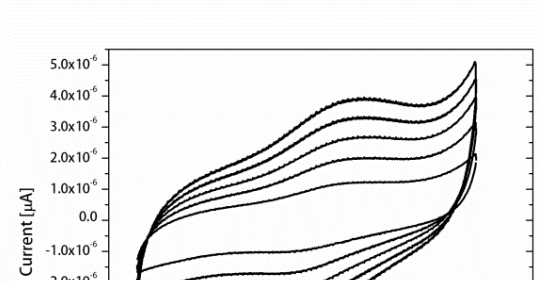

(B)

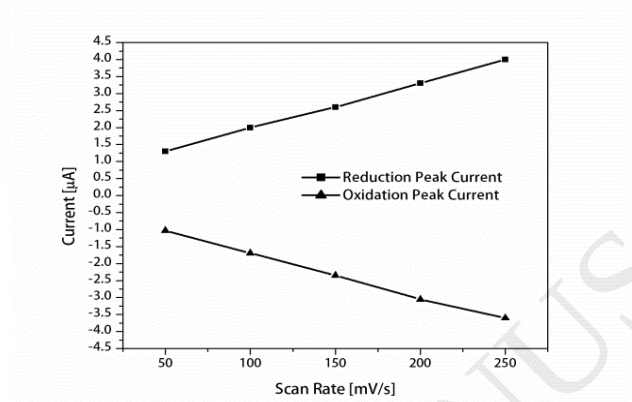

(C)

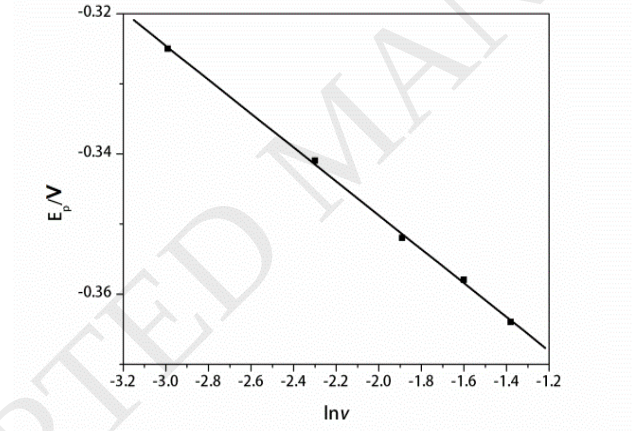

Figure 3. (A) Cyclic voltammamograms of the Au/SAM/HRP/CNT electrode with different scan rates in 0.1 mol l^{-1} PBS with pH 7.0. The scan rates were from 0.05 to 0.25 V/s. (B) Reduction and oxidation peak current verses scan rates based on fig.3A. (C) Relationship between the cathodic peak potential (E_p) and the natural logarithm of scan rate (ln v) for the Au/SAM/HRP/CNT electrode.

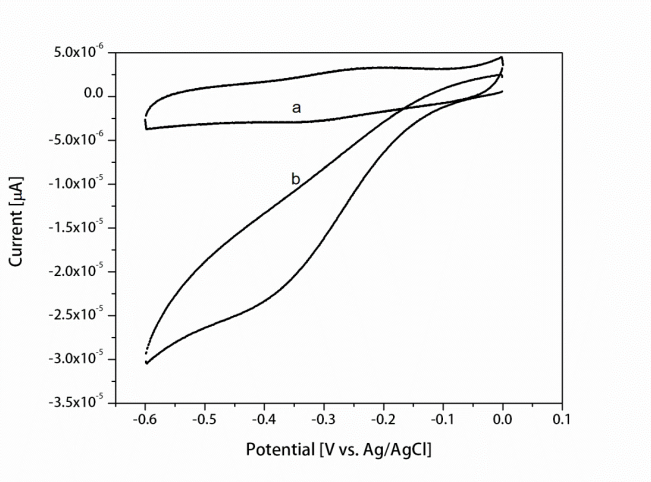

Figure 4. Cyclic voltammograms of the Au/SAM/HRP/CNT electrode in the absence of H_2O_2 (a) and in the presence (b) of 5×10^{-6} M in PBS with pH 7.0 at the scan rate of 0.2 V/s.

(A)

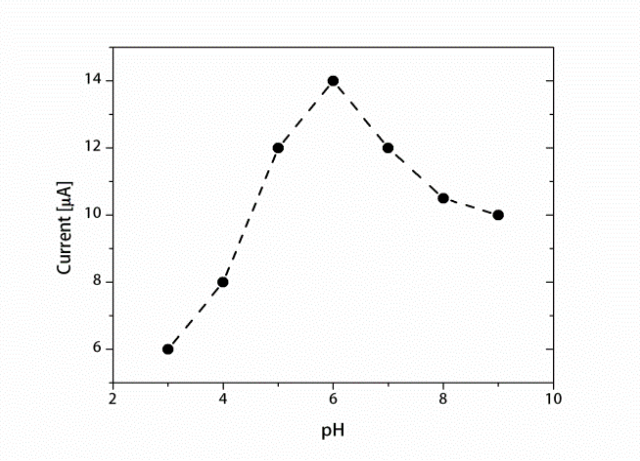

(B)

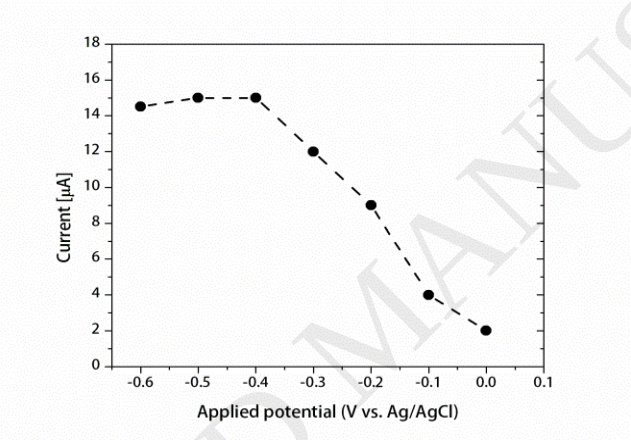

Figure 5. (A) Effect of amperometric current responses of the Au/SAM/HRP/CNT electrode at different applied potentials measured in a pH 7.0 PBS containing 5×10^{-5} mol l^{-1} H_2O_2 (B) Relationship between pH and the catalytic current of the Au/SAM/HRP/CNT electrode in the presence of 5×10^{-5} mol l^{-1} H_2O_2 in PBS at the potential of -0.4 V.

(A)

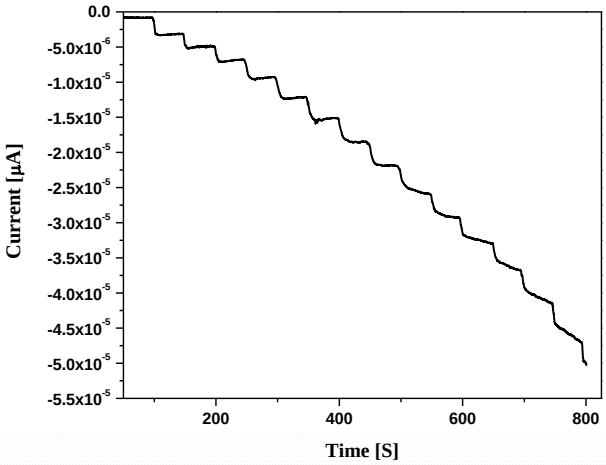

(B)

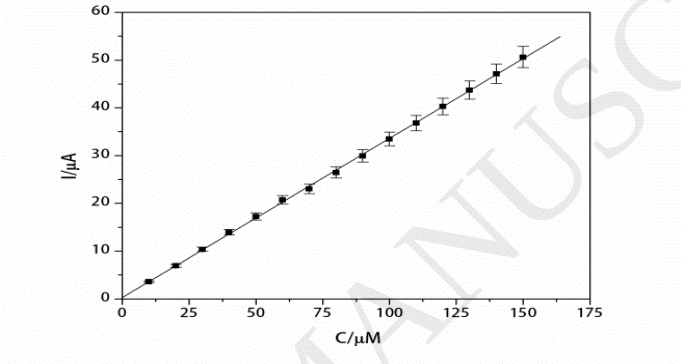

(C)

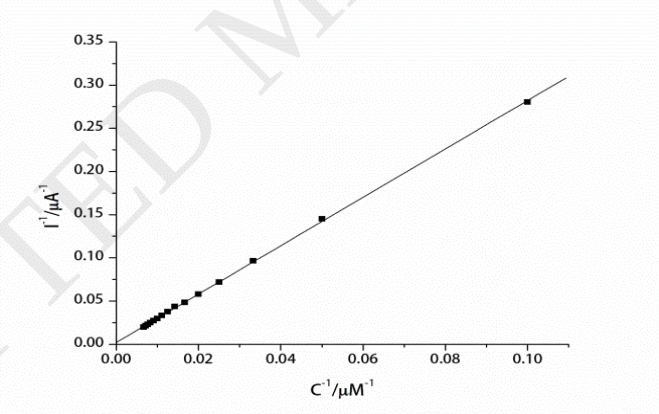

Figure 6. Typical Steady-state amperometric response of the Au/SAM/HRP/CNT (a); with the successive additions of 5×10^{-6} mol l^{-1} H_2O_2 in 0.1 mol l^{-1} PBS (pH 6.0).at the operating potential of -0.4 V. (B) Calibration plot for the Au/SAM/HRP/CNT electrode in the same experimental conditions as Figure 5. (C) the Lineweaver–Burk plot of $1/I_{ss}$ vs. 1/C.

Modified Electrode	Linear range	LOD	Stability	Ref.
HRP in Au nano-seed	4.1×10^{-5} to 6.3×10^{-4} M	5.9 µM	90% 14 days	31
HRP in Carbon nanotube	3×10^{-5} to 1×10^{-2} M	12.89 µM	Not reported	32
HRP in nano-Au with polymer.	4.2×10^{-7} to 1.5×10^{-3} M	0.17	84.5% (30 days)	33
HRP in nano-Au on GC electrode	1.22×10^{-5} to 1.1×10^{-3} M	6.1	70% (35 days)	34
HRP in SAM-nano Au	2.6×10^{-6} to 8.8×10^{-3} M	0.64 µM	70%(14 days)	35
HB in crosslinked 3D networks	3×10^{-6} to 2×10^{-4} M	0.5 µM	90% (21 days)	19
In this work (HRP in crosslinked 3D networks)	3×10^{-7} to 1.2×10^{-4} M	0.022 µM	90% (21 days)	

Table 1. Comparison of the performance of different H_2O_2 biosensors (HRP = Horseradish peroxide; LOD = Limit of Detection).